

# Measured decrease in T1 relaxation time in skeletal muscle on oxygen inhalation

D. McGrath<sup>1</sup>, J. Naish<sup>1</sup>, P. Beatty<sup>1</sup>, A. Jackson<sup>1</sup>, J. Waterton<sup>2</sup>, C. Taylor<sup>1</sup>, G. Parker<sup>1</sup>

<sup>1</sup>Imaging Sciences and Biomedical Engineering, University of Manchester, Manchester, Lancashire, United Kingdom, <sup>2</sup>AstraZeneca, Alderley Park, Macclesfield, Cheshire, United Kingdom

## INTRODUCTION

Dissolved oxygen can be used as a contrast agent in MRI due to the paramagnetic properties of the oxygen molecule. A modest increase in the longitudinal relaxation rate  $R_1 \equiv T_1^{-1}$  of water protons is induced by  $O_2$ , and the increase is proportional to the dissolved oxygen concentration. Measurements of oxygenation using these effects can provide an indication of tissue perfusion and metabolism and has been tested in various organs and tissues ((1)-(6)). We discovered that contrary to previous findings, the  $T_1$  of skeletal muscle is reduced significantly in hyperoxic conditions. We also obtained measures of the time course of regional signal intensity change for healthy skeletal muscle during oxygen wash-in and wash-out.

## METHODS

The images used in this study (3) were obtained from five normal volunteers, with written informed consent (two males, three females, ages 30-39), using a 1.5T Philips Gyroscan NT Integra MR system (Philips Medical Systems, Best, Netherlands) and were primarily designed to measure the effect of dissolved oxygen on  $T_1$  times in the lungs. Subjects breathed medical air or 100% oxygen through an MR compatible Bain breathing system (Intersurgical Ltd., Wokingham, UK) and tightly fitting mask. A standard anaesthesia trolley (10 l/min capability) was used. A first set of images was acquired in order to measure  $T_1$  during air-breathing. A half Fourier single shot turbo spin-echo (HASTE) sequence was used with 68 phase encoding steps and inter-echo spacing of 4ms, effective echo time 16ms,  $128 \times 128$  matrix with field of view 450mm, coronal section with slice thickness 10mm.  $T_1$  measurements were performed using a saturation recovery HASTE sequence with saturation times ( $T_{SAT}$ ) of 100, 200, 400, 800, 1200, 1700, 2300, 3000, 3500 ms. Five images were collected for each saturation time to enable averaging over the cardiac cycle. Saturation recovery (SR) was chosen above inversion recovery (IR), to give a shorter total imaging time (TR can be reduced), i.e. approximately 2.5min for the set of 45 images used. Next, dynamic image acquisitions were performed to measure the characteristic wash-in and wash-out times ( $t_c$ ) for pure oxygen using an IR HASTE sequence with an inversion time of 720ms (chosen to approximately null the signal from the lungs while breathing air (7)). The gas supply was switched from medical air to 100% oxygen after the tenth image in the series. A set of  $T_1$  measurement SR images was acquired while the subject continued to breathe 100% oxygen at the same coronal location. Finally a second series of dynamic images was acquired with the gas supply being switched back to medical air after the tenth image. The whole set of measurements for a single coronal slice took approximately 12 minutes. Regions of interest were drawn on the left and right posterior rotator cuff shoulder muscles (best visible skeletal muscle group) inside a margin of approximately 2 pixels of the identifiable muscle boundaries. Average  $T_1$  values for the regions were calculated for air and oxygen using each set of 45 varying  $T_{SAT}$  images by fitting the average over the region of interest to an exponential of the form in equation 1 (see below), where  $S(T_{SAT})$  is the average pixel intensity at each  $T_{SAT}$  and  $A$  and  $B$  are constants using a Levenberg-Marquardt fitting algorithm. The fitting was repeated for the 100% oxygen image sets. Using the dynamic image acquisitions, oxygen wash-in and wash-out times were calculated by fitting with the same algorithm an exponential of the form in equation 2 where  $S(t)$  is the average signal intensity of the region at time  $t$ ,  $t_c$  is the characteristic wash-in (or wash-out) time and  $\alpha$  and  $\beta$  are constants. For the fitting routine the time corresponding to  $t=0$  was set as the time of the first image after the initial 10 baseline images. The standard deviation of the mean signal intensity from the muscle region of interest in the air-breathing baseline ten images was used to estimate the error on each data point for the fitting routine.

## RESULTS

$T_1$  values, and estimated errors on the fit, for the left and right posterior rotator cuff muscle during air and oxygen inhalation are given in table 1. The values at the end of each column are the mean and standard deviation. The value of  $T_1$  for skeletal muscle during air-breathing is consistent with values quoted in literature, (8), for skeletal muscle. As an added reference, the value for normoxic  $T_1$  in liver was measured at  $690 \pm 120$ ms and in spleen at  $1430 \pm 330$ ms, and these values are also consistent with those in literature (4, 8). Although the difference between  $T_1$  for air-breathing and oxygen-breathing in muscle is small, it is statistically significant (using the paired  $t$ -tailed Student  $t$  test,  $P=0.00073$ ). To support this finding, there is no statistically significant difference between the  $T_1$  values for the left and right muscle regions on air inhalation, and likewise for the left and right region values on oxygen inhalation.

The decrease in  $T_1$  in hyperoxia is further confirmed by the dynamic data. Figure 1 illustrates example time courses of oxygen wash-in and wash-out for the posterior rotator cuff muscle in one volunteer, clearly indicating an increased signal due to a decrease in  $T_1$  on wash-in, and a decreased signal due to an increased  $T_1$  on wash-out. There exists a pattern of noise along these curves which appears to follow the progress of the breathing cycle. This may be in part due to slight movement of the muscle in and out of the coronal plane or sub-pixel motion within the coronal plane, effects such as varying blood flow in the muscle, or varying degrees of low-level motion-induced artefact. Table 2 gives the  $t_c$  values obtained from the model fitting of the dynamic sequence for left side and right side posterior rotator cuff muscles and the estimated error on the fit. The values at the end of the columns are mean  $\pm$  standard deviation. The wash-out times were not significantly different from the wash-in times ( $P=0.30265$ , paired Student  $t$  test, 2-tailed). Also, the wash-in  $t_c$  times for the left muscles were not significantly different from those for the right muscles and likewise for the wash-out  $t_c$  times.

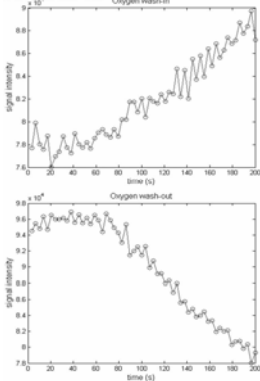
## DISCUSSION AND CONCLUSION

Contrary to previous findings (5, 6), we have measured a significant decrease in  $T_1$  for skeletal muscle. Possible explanations include that the posterior rotator cuff muscles may differ from the muscle groups used in (5) and (6) (i.e. dorsal back and calf muscles respectively) in terms of blood flow, regional oxygen consumption, or residence time in the vasculature during passage from the lungs. We have measured characteristic oxygen wash-in and wash-out times for the posterior rotator cuff muscle. The variation in these values between subjects could be due to inter-individual variation in factors such as oxygen supply in the scanner, lung function, heart rate, and muscle perfusion. These initial baseline results provide an indication of the behaviour of healthy muscle tissue in response to breathing 100% oxygen, and could be used to evaluate oxygen delivery and consumption in skeletal muscle in diseases such as myopathies, metabolic diseases, peripheral vascular disease and cancer cachexia. OE-MRI has the advantages of being non-invasive, non-ionising, relatively high-resolution and inexpensive, requiring little specialist equipment or procedures.

## REFERENCES

- Young IR et al, *J Comp Assisted Tomography*, 1981;5:543-547.
- Edelman RR et al, *Nat Med*, 1996;2(11):1236-1239.
- Naish JH et al, *Magn Reson Med*, 2005;54(2):464-469.
- Jones RA et al., *Magn Reson Med*, 2002;47:728-735.
- Tadamura E et al, *J Magn Reson Imaging*, 1997;7(1).
- Noseworthy MD et al., *J Magn Reson Imaging*, 1999;9:814-820.
- Ohno Y et al., *Magn Reson Med*, 2002;47(6):1139-1144.
- de Certaines JD et al., *Magn Reson Imaging*, 1993;11(6):841-850.

Figure 1:



$$\text{Eq. (1): } S(T_{SAT}) = A - B \exp\left(-\frac{T_{SAT}}{T_1}\right)$$

$$\text{Eq. (2): } S(t) = \alpha - \beta \exp\left(-\frac{t}{t_c}\right)$$

Table 1:

Subject	$T_1$ Air (ms)		$T_1$ 100% $O_2$ (ms)	
	Left Side	Right Side	Left Side	Right Side
1	1082 ± 83	1179 ± 92	1045 ± 81	1090 ± 86
2	1088 ± 71	1020 ± 57	1070 ± 70	964 ± 54
3	1100 ± 90	1249 ± 110	1043 ± 86	1126 ± 100
4	1007 ± 70	948 ± 60	1001 ± 70	923 ± 59
5	1148 ± 96	1586 ± 140	1080 ± 92	1454 ± 140
Mean	1085 ± 51	1196 ± 249	1047 ± 31	1111 ± 209
Overall Mean	1140 ± 179*		1080 ± 145*	

Table 2:

Subject	$t_c$ wash-in (s)		$t_c$ wash-out (s)	
	Left Side	Right Side	Left Side	Right Side
1	99 ± 20	119 ± 43	77 ± 15	113 ± 37
2	146 ± 62	144 ± 100	129 ± 38	108 ± 45
3	81 ± 12	106 ± 40	96 ± 16	111 ± 27
4	123 ± 37	91 ± 50	114 ± 40	107 ± 30
5	114 ± 34	89 ± 60	100 ± 12	98 ± 34
Mean	113 ± 25	110 ± 23	103 ± 20	107 ± 6
Overall Mean	111 ± 22*		105 ± 14*	